PROCEEDINGS OF SPIE

SPIEDigitalLibrary.org/conference-proceedings-of-spie

Enhanced dissipative sensing in a microresonator with multimode input (experiment)

Rajagopal, Sreekul Raj, Rosenberger, A. T.

Sreekul Raj Rajagopal, A. T. Rosenberger, "Enhanced dissipative sensing in a microresonator with multimode input (experiment)," Proc. SPIE 11296, Optical, Opto-Atomic, and Entanglement-Enhanced Precision Metrology II, 112963Q (25 February 2020); doi: 10.1117/12.2556503

SPIE.

Event: SPIE OPTO, 2020, San Francisco, California, United States

Downloaded From: https://www.spiedigitallibrary.org/conference-proceedings-of-spie on 20 Mar 2020 Terms of Use: https://www.spiedigitallibrary.org/terms-of-use

Enhanced dissipative sensing in a microresonator with multimode input (experiment)

Sreekul Raj Rajagopal and A. T. Rosenberger*
Department of Physics, Oklahoma State University, Stillwater, OK, USA 74078-3072

ABSTRACT

Optical whispering-gallery mode (WGM) microresonators have proven their ability to enhance light-matter interaction and hence are widely used for sensing. In contrast to the traditional approach of using symmetric adiabatic tapers to couple light into the resonators, we use an asymmetric non-adiabatically tapered fiber to couple light from two fiber modes into a microresonator. Previously it was shown that dissipative sensing of an absorbing analyte can be more sensitive than dispersive sensing, and that dissipative sensing based on dip depth change can be more sensitive than dissipative sensing based on linewidth change. In this report, we demonstrate an enhancement in sensitivity by three orders of magnitude for dissipative sensing based on dip depth change. The enhancement factor is independent of the quality factor *Q* of the WGM and is determined solely by the values of the throughput power in the absence of analyte when the two fiber modes are in and out of phase at the point where they couple into the WGM.

Keywords: microresonator, whispering-gallery modes, dissipative sensing, asymmetric tapered fibers.

1. INTRODUCTION

In the past few decades, due to their high quality factors and small mode volumes, optical whispering-gallery mode (WGM) microresonators have proven to be an exceptional platform for the advancement of optical sensors.[1] Recently, WGM optical sensors have achieved ultrahigh sensitivity and low limit of detection in detecting changes in various physical quantities.[2,3] Optical WGM sensors rely on two sensing principles, dispersive and dissipative sensing.[4,5] Dispersive sensing is based on the shift in WGM resonance frequency with a change in the refractive index of the surrounding medium whereas dissipative sensing, in general, depends on the change in linewidth induced by a lossy (absorbing) analyte. In addition to the change in linewidth, the introduction of a lossy analyte into the surrounding environment of an optical WGM sensor will also induce a change in the resonant throughput dip depth. Hence a comprehensive study on dissipative sensing can be performed by detecting the change in the resonant throughput dip depth of a WGM.

Dissipative sensing based on dip depth change can provide a better limit of detection than frequency shift measurements.[6,7,8] Recently a novel approach for improving the limit of detection for the dip depth based dissipative sensing was proposed.[9,10] Usually adiabatic tapered fibers[11] are used to couple light in and out of the microresonators. Hence a single mode is incident on the microresonator. The proposed scheme for improving the limit of detection depends on having multiple modes incident on the microresonator using a non-adiabatic tapered fiber.

2. CRITERIA FOR ADIABATIC AND NON-ADIABATIC TAPERS

Tapered optical fibers are used to couple light efficiently into microresonators. A tapered fiber is made by stretching a heated optical fiber, and it consists of a narrow stretched filament called the taper waist, each end of which is linked to the unstretched fiber by a section known as the taper transition.

A taper transition is said to be adiabatic if light in the single mode of the untapered fiber couples only to the HE_{11} mode at the taper waist. On the contrary, a taper transition is said to be non-adiabatic if light in the single mode of the untapered fiber also couples to higher order fiber modes at the taper waist.

*atr@okstate.edu; phone 1 405 744-6742; fax 1 405 744-6811; rosenberger.okstate.edu

Optical, Opto-Atomic, and Entanglement-Enhanced Precision Metrology II, edited by Selim M. Shahriar, Jacob Scheuer, Proc. of SPIE Vol. 11296, 112963Q · © 2020 SPIE
CCC code: 0277-786X/20/$21 · doi: 10.1117/12.2556503

Downloaded From: https://www.spiedigitallibrary.org/conference-proceedings-of-spie on 20 Mar 2020
Terms of Use: https://www.spiedigitallibrary.org/terms-of-use

The local cladding taper angle Ω_{cl} is defined as the angle between the fiber axis and the tangent to the taper profile at the point of interest. Comparing Ω_{cl} to a suitably defined maximum value $\Omega_{\max}$ at each point z of the taper transition region can be used as a tool to investigate the conditions for adiabatic and non-adiabatic tapering.[12] If the taper transition is adiabatic,

$$\Omega_{cl}(z) \approx \left| \frac{dr_{cl}(z)}{dz} \right| << \left(\beta_f(z) - \beta_h(z)\right) r_{cl}(z), \tag{1}$$

where r_{cl} is the local cladding radius, and β_f and β_h are the propagation constants of the fundamental and the higher order mode. For the taper to be adiabatic, we define the maximum cladding taper angle to be

$$\Omega_{\max}(z) = \frac{r_{cl}(z)\left(\beta_f(z) - \beta_h(z)\right)}{2\pi} = \frac{r_{cl}}{z_b}, \tag{2}$$

where z_b is the beat length of the two fiber modes. The "flame brush" technique is used to fabricate tapered fibers in our lab. An optical fiber with its jacket removed is attached to two motorized translation stages. Underneath the stripped area of the fiber a hydrogen torch is installed on another motorized translation stage and the hydrogen flame continuously brushes the stripped fiber along its length back and forth over a distance known as the brushing length at a higher constant speed. In order to produce an asymmetric tapered fiber, the two motorized stages are pulled with different speeds, whereas an adiabatic tapered fiber is fabricated by pulling the motorized stages with the same speed. Plots of taper angles as functions of inverse taper ratio r_{cl}/r_0 where r_0 is the cladding radius of the original fiber, corresponding to both adiabatic and non-adiabatic tapered fibers made in our lab, are shown in Fig. 1.

For all values of inverse taper ratio, an adiabatic taper will have a taper angle Ω_{cl} which is always less than the delineation curve defined by the larger of $\Omega_{\max}$ for core guidance and $\Omega_{\max}$ for cladding guidance, whereas for a non-adiabatic taper the plot of the taper angle will pass above the delineation curve for at least some values of the inverse taper ratio as shown in Fig. 1(b).

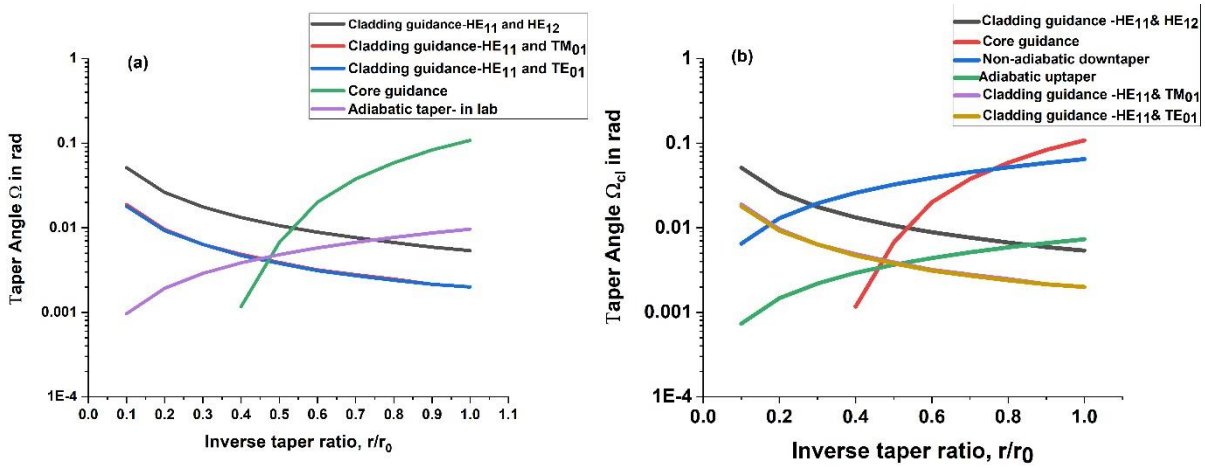

Fig. 1. Delineation curve for different taper profiles. (a) Adiabatic taper. (b) Non-adiabatic and adiabatic tapers.

For a tapered fiber with a waist diameter of $2\,\mu m$, in addition to the fundamental mode HE_{11}, other modes such as TE_{01}, TM_{01}, HE_{21}, EH_{11}, HE_{31}, and HE_{12} can also be excited. The propagation constants of TE_{01}, TM_{01}, and HE_{21} are very close to each other and so the three modes can be considered as one - LP_{11}. Hence their corresponding delineation curves (blue/red in Fig. 1(a) and yellow/purple Fig. 1(b)) lie on top of each other. In Fig. 1(a) the green curve represents the delineation curve assuming core guidance whereas the delineation curves assuming cladding guidance are represented by the blue/red and black (HE_{12}, which dominates the last three modes) curves. The purple curve representing the taper angles of a typical symmetric adiabatically tapered fiber fabricated in our lab passes below the intersection of the delineation curves defined by blue/red (lowest possible) and green curves with some round off at the

Downloaded From: https://www.spiedigitallibrary.org/conference-proceedings-of-spie on 20 Mar 2020
Terms of Use: https://www.spiedigitallibrary.org/terms-of-use

intersection. This suggests that the fabricated tapered fiber has adiabatic down and up taper transitions. For an asymmetric taper as in Fig. 1(b), based on beat length measurements it was found that HE_{11} and LP_{11} are the modes that are excited, and hence the corresponding delineation curves (yellow/purple and red curves) with some round off at the intersection are used to differentiate between an adiabatic and a non-adiabatic taper transition. In Fig. 1(b) the red curve represents the delineation curve assuming core guidance. (The black curve would be used as the delineation curve for cladding guidance if HE_{12} were the other excited mode.) For the blue curve in Fig. 1(b), the downtaper angles are above this intersection, which indicates that the downtaper will be non-adiabatic. The green curve representing the uptaper angles passes barely below the intersection of the delineation curves, indicating that the uptaper is adiabatic. Figure 1(b) thus suggests that the fabricated asymmetric tapered fiber has a non-adiabatic taper transition on one side and an adiabatic taper transition on the other side.

For an asymmetric tapered fiber coupled microresonator system, the throughput spectral profile of a WGM mode can be asymmetric depending on the relative phase and amplitude of the incident fiber modes. Previously it was reported that by using an asymmetric tapered fiber coupled microresonator system, it is possible to obtain Fano resonances which can be used for enhancement of frequency-shift sensing.[13]

2. THEORY

The behavior of a asymmetrically tapered fiber-coupled microresonator system can be explained adequately using a simplified model. In this model, the two fiber modes are considered as two orthogonal (spatially, not in polarization) guided waves incident on the microresonator, having the same frequency but different propagation constants and thus an adjustable relative phase β. The amplitudes of the two incident fiber modes at the point where light gets coupled into the microresonator are given by E_{i1} and $E_{i2}e^{i\beta}$ respectively. The two incident fiber modes couple into a single whispering-gallery mode of the resonator as shown in Fig. 2. At the taper waist, the outcoupled light is shared by the two fiber modes whose amplitudes are given by E_{r1} and E_{r2}. Since the uptaper is adiabatic, there is no energy transfer between the fiber modes and only the first of the fiber modes namely E_{r1}, is captured as measurable throughput.

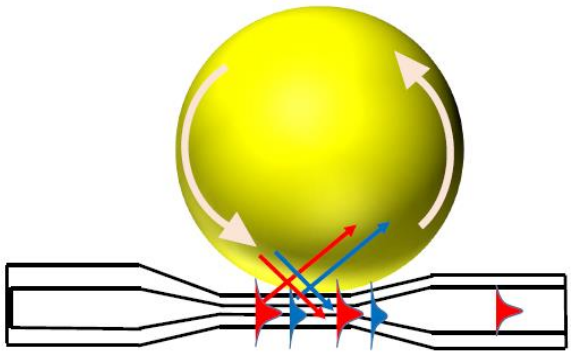

Fig. 2. Asymmetric tapered fiber and a microresonator in contact. The two fiber modes, fundamental (red) and higher order (blue) get coupled into a single whispering-gallery mode. The WGM couples out into both fiber modes. The higher order mode gets lost and only the fundamental mode is captured in the detector.

On resonance, the ratio of throughput power to input power can be expressed as

$$R_{0\beta} = \frac{(T_1 - T_2 - \alpha L)^2 + 4T_1T_2m^2 + 4(T_1 - T_2 - \alpha L)\sqrt{T_1T_2}\,m\cos\beta}{(T_1 + T_2 + \alpha L)^2}, \tag{3}$$

Downloaded From: https://www.spiedigitallibrary.org/conference-proceedings-of-spie on 20 Mar 2020
Terms of Use: https://www.spiedigitallibrary.org/terms-of-use

where T_1, T_2 represent the strengths of coupling of the fiber modes to the WGM, αL represents the intrinsic power loss per round trip, and m represents the ratio of amplitude moduli of the incident fiber modes. The relative throughput dip depth is given by

$$M = 1 - R_{0\beta} = \frac{4T_1(T_2 + \alpha L) - 4T_1T_2m^2 - 4(T_1 - T_2 - \alpha L)\sqrt{T_1T_2}\, m\, \cos\beta}{(T_1 + T_2 + \alpha L)^2}. \tag{4}$$

Upon adding analyte if the change in dip depth is small, then

$$\frac{1}{M}\frac{dM}{d\alpha L} = \frac{T_1(T_1 - T_2 - \alpha L) + 2T_1T_2m^2 + (2T_1 - T_2 - \alpha L)\sqrt{T_1T_2}\, m\cos\beta}{(T_1 + T_2 + \alpha L)\left\{T_1(T_2 + \alpha L) - T_1T_2m^2 - (T_1 - T_2 - \alpha L)\sqrt{T_1T_2}\, m\cos\beta\right\}}. \tag{5}$$

Now instead of using an asymmetrically tapered fiber with a non-adiabatic downtaper, if an adiabatically tapered fiber of the same waist diameter is used to couple light into and out of the microresonator, then the corresponding relative throughput dip depth and its fractional change can be found by substituting $m = 0$ in Eq. (4) and Eq. (5).

Thus the sensitivity enhancement factor is given by the ratio of Eq. (5) with m to Eq. (5) with $m = 0$:

$$\eta = \left| \frac{(T_2 + \alpha L)\left[T_1(T_1 - T_2 - \alpha L) + 2T_1T_2m^2 + (3T_1 - T_2 - \alpha L)\sqrt{T_1T_2}\, m\, \cos\beta\right]}{(T_1 - T_2 - \alpha L)\left\{T_1(T_2 + \alpha L) - T_1T_2m^2 - (T_1 - T_2 - \alpha L)\sqrt{T_1T_2}\, m\, \cos\beta\right\}} \right|. \tag{6}$$

Based on the above equations, a numerical model which uses as input experimentally measured linewidth $\Delta\upsilon$, microresonator radius a, and relative throughput when the fiber modes are in phase ($\beta = 0$) and out of phase ($\beta = \pi$) was developed and explained in our previous work.[9]

3. EXPERIMENTAL PROCEDURE AND RESULTS

The internal evanescent fraction of the hollow bottle resonator (HBR) can be greater than the external evanescent fraction thereby making the HBR an ideal candidate for performing internal sensing.[1,14] In our previous work a cost effective way of fabricating the HBR[15] and its usage as a chemical absorption sensor were reported.

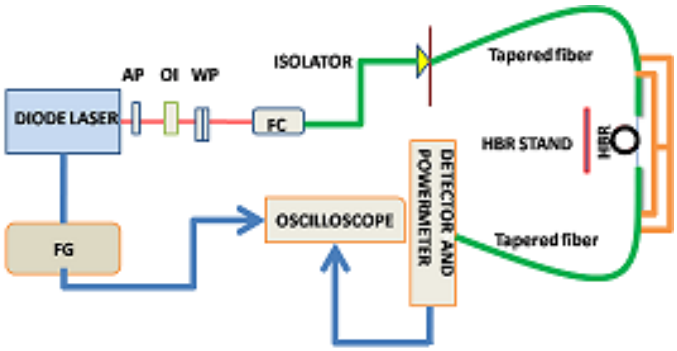

Fig. 3. Experimental setup used for dye sensing.

An illustration of the experimental setup for dye absorption sensing is shown in Fig. 3. WGMs of the HBR are excited by the light from a tunable diode laser (1508-1585 nm) which is frequency scanned using a function generator (FG). The free-space laser beam travels through an anamorphic prism (AP), an optical isolator (OI), a set of waveplates (WP), the fiber coupler (FC), and an optical fiber isolator before it gets coupled to the tapered fiber.

Light is coupled in and out of the microresonator using an asymmetrically tapered fiber. Under the right conditions, upon translating the microresonator along the fiber waist, the throughput of WGMs changes from peak to dip in a periodic manner and thus the beat length was measured. From the beat length measurements, it was found that the excited higher order mode was LP_{11} and not HE_{12}. According to our model predictions, when the throughput profile of a

Downloaded From: https://www.spiedigitallibrary.org/conference-proceedings-of-spie on 20 Mar 2020
Terms of Use: https://www.spiedigitallibrary.org/terms-of-use

WGM changes upon translation from a small peak to a shallow dip in a periodic manner, the indication is that the WGM is a candidate for maximum sensing enhancement.

When the fiber modes were in phase, predetermined concentrations of analyte (dye) was added to the methanol filled HBR and changes in WGM dip depths were recorded. The corresponding throughput spectra for one case are shown in Fig. 4. Then the asymmetric tapered fiber was replaced by a symmetric adiabatic tapered fiber of the same waist diameter and changes in dip depths with concentration, for the same WGM, were again recorded.

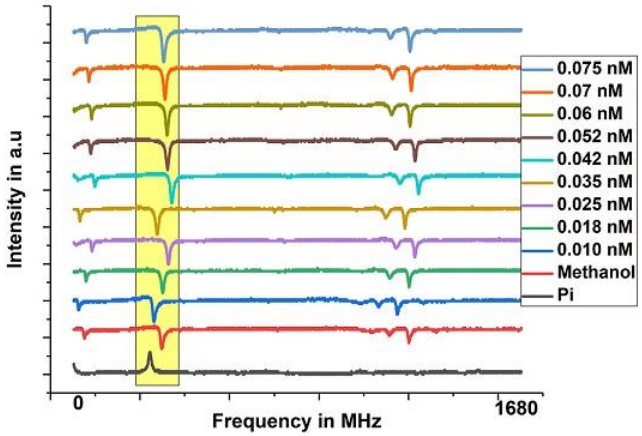

Fig. 4. Throughput spectra with upward shift indicating higher analyte concentrations. Bottom trace for methanol only, $\beta = \pi$.

For the case illustrated above, knowing $R_{00} = 0.92$ and $R_{0\pi} = 1.02$ allows us to predict an enhancement factor[16] of 948. Knowing the values of R_{00} and $R_{0\pi}$ along with linewidth $(\Delta\upsilon)$ allows us to compute T_1, $T_2 + \alpha L$, and $T_2 m^2$ and hence the relative throughput dip depth of the mode using Eq. (4). The internal evanescent fraction f of the WGM was determined to be 0.195 by fitting multiple dip depths for different analyte concentrations. Consequently knowing f and the absorption coefficient of the analyte enables us to calculate the theoretical dip depth and hence the theoretical relative dip depth change $\left(\frac{\Delta M}{M}, \frac{dM}{M}\right)$ as a function of analyte concentrations for both cases where asymmetric and symmetric tapered fibers (of the same waist radius) are used to couple light into and out of the microresoantor. With the symmetric tapered fiber, the mode of interest gets closer to critical coupling. Thus any measurable change in dip depth is possible only at high concentrations and the corresponding change in fractional dip depth at low concentrations can be estimated by extrapolation. The theoretical and experimental results are plotted in Fig. 5.

According to theory, for both multiple and single fiber mode/s incident on the microresonator, in the linear regime (at very low concentrations) $\frac{\Delta M}{M}$ and $\frac{dM}{M}$ are equal. The theory predicts that for the multiple-mode-incident scenario, as the concentration increases, $\frac{\Delta M}{M}$ gets smaller as compared to $\frac{dM}{M}$ whereas with a single mode incident (adiabatic taper), $\frac{\Delta M}{M}$ gets larger as compared to $\frac{dM}{M}$. A very similar trend is shown in Fig. 5, 6, and 7. The blue curve in Fig. 5(a) represents the experimental curve which agrees very well with the theoretical predictions at low concentrations. At high concentrations, the experimental curve doesn't agree well with the theoretical prediction. This may be due to the uncertainty in measuring the throughput power when the fiber modes are in and out of phase and also due to the uncertainty in the concentration of analyte inside the HBR. Two other sets of results corresponding to enhancements of 1298 and 397 are shown in Fig. 6 and Fig. 7. All three are summarized in Table 1; as Figs. 5-7 show, the measured experimental enhancement at low analyte concentration is equal to the predicted enhancement.

Downloaded From: https://www.spiedigitallibrary.org/conference-proceedings-of-spie on 20 Mar 2020
Terms of Use: https://www.spiedigitallibrary.org/terms-of-use

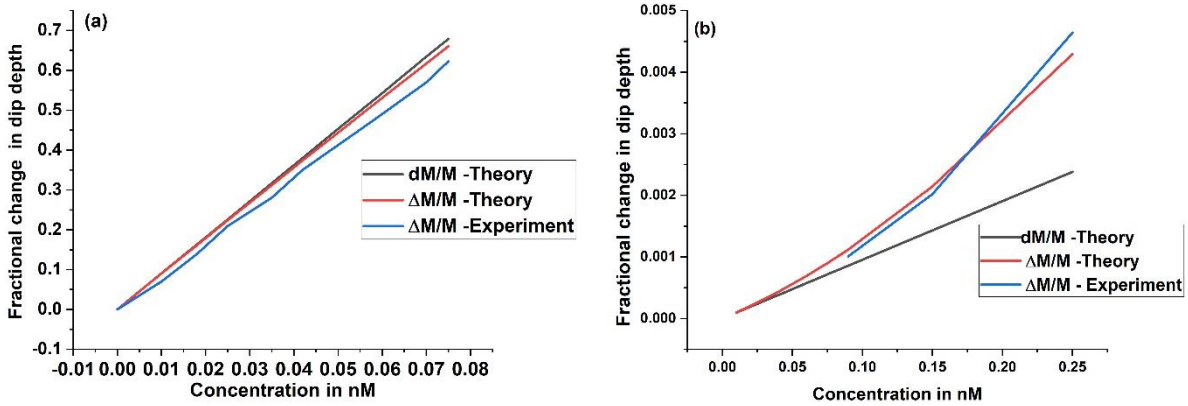

Fig. 5. Theoretical and experimental fractional dip depth for the same WGM excited by (a) asymmetric tapered fiber, (b) adiabatic tapered fiber. The enhancement factor $\eta = 948$ and evanescent fraction $f = 0.195$.

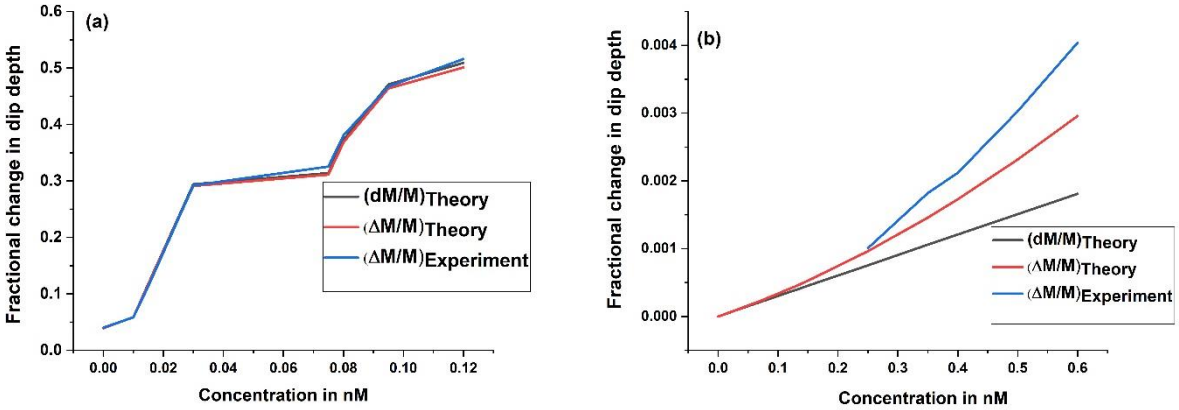

Fig. 6. Theoretical and experimental fractional dip depth for the same WGM excited by (a) asymmetric tapered fiber, (b) adiabatic tapered fiber. The enhancement factor $\eta = 1298$ and evanescent fraction $f = 0.07$.

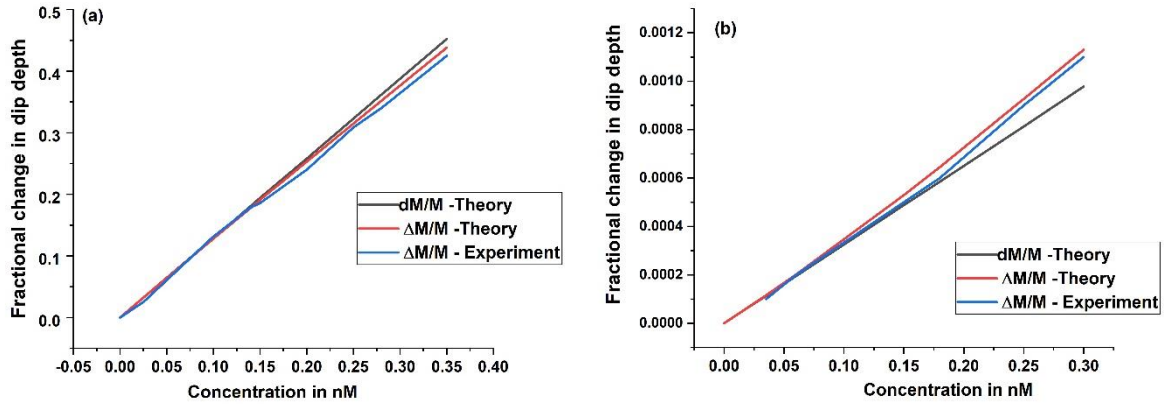

Fig. 7. Theoretical and experimental fractional dip depth for the same WGM excited by (a) asymmetric tapered fiber, (b) adiabatic tapered fiber. The enhancement factor $\eta = 398$ and evanescent fraction $f = 0.19$.

Downloaded From: https://www.spiedigitallibrary.org/conference-proceedings-of-spie on 20 Mar 2020
Terms of Use: https://www.spiedigitallibrary.org/terms-of-use

Table 1. Summary of experimental results

R_{00}	$R_{0\pi}$	f	η
0.92	1.02	0.195	948
0.94	1.04	0.070	1298
0.87	1.01	0.190	398

4. DISCUSSION

In this report, we provide experimental evidence for enhancement in dissipative sensing by using an asymmetric tapered fiber to couple light into the microresonator. An absorbing dye dissolved in methanol is used as the detected analyte, interacting with the internal evanescent fraction of a whispering-gallery mode in a hollow bottle resonator. The asymmetrically bitapered fiber has a non-adiabatic downtaper, allowing excitation of two modes of the fiber waist, while its adiabatic uptaper ensures that only the fundamental mode survives to provide measurable throughput. To quantify the sensing enhancement, a model was developed that compares the relative change in throughput dip depth to the relative dip depth change observed with an adiabatic (single incident mode) tapered fiber of the same waist radius. In the linear regime (low analyte concentration), with multiple fiber modes incident, the enhancement factor predicted by the model depends only on R_{00} and $R_{0\pi}$.[16] The experimental enhancement measured by comparing the dip depth signal from two fibers, one asymmetric and one adiabatic, agrees well with the model predictions. The model also gives a specific prediction of how much better the sensitivity is that can be achieved with changes in dip depth as compared to changes in linewidth,[16] and experiments to test this are underway.

REFERENCES

[1] Foreman, M. R., Swaim, J. D., and Vollmer, F., "Whispering gallery mode sensors," Adv. Opt. Photon. 7, 168- 240 (2015).

[2] Shen, B. Q., Yu, X. C., Zhi, Y., Wang, L., Kim, D., Gong, H. Q., and Xiao, Y. -F., "Detection of single nanoparticles using the dissipative interaction in a high-Q microcavity," Phys. Rev. Appl. 5, 024011 (2016).

[3] Shopova, S. I., Rajmangal, R., Holler, S., and Arnold, S., "Plasmonic enhancement of a whispering-gallery-mode biosensor for single nanoparticle detection," Appl. Phys. Lett. 98, 243104 (2011).

[4] Vollmer, F., and Yang, L., "Review label-free detection with high-Q microcavities: a review of biosensing mechanisms for integrated devices," Nanophotonics 1(3-4), 267-291 (2012).

[5] Yang, Y., Madugani, R., Kasumine, Sho., Ward, J. M., and Nic Chormaic, S., "Cavity ring-up spectroscopy for dissipative and dispersive sensing in a whispering gallery mode resonator," Appl. Phys. B 122, 291 (2016).

[6] Rosenberger, A. T., "Analysis of whispering-gallery microcavity-enhanced chemical absorption sensors," Opt. Express 15, 12959-12964 (2007).

[7] Ren, H., Zou, L. C., Liu, Z., Le, Z., Qin, Y., Guo, S., and Hu, W., "Dissipative sensing with low detection limit in a self-interference microring resonator," J. Opt. Soc. Am. B 36, 942-951 (2019).

[8] Farca, G., Shopova, S. I., and Rosenberger, A. T., "Cavity-enhanced laser absorption spectroscopy using microresonator whispering-gallery modes," Opt. Express 15, 17443-17448 (2007).

[9] Rosenberger, A. T., "Absorption sensing enhancement in a microresonator coupled to a non-adiabatic tapered fiber," Proc. SPIE 10548, 105480G (2018).

[10] Rajagopal, S. R., Ke, L., and Rosenberger, A. T., "Enhanced absorption sensing using a non-adiabatic tapered fiber coupling to a whispering-gallery microresonator," Proc. SPIE 10904, 109041D (2019).

[11] Birks, T. A., and Li, Y. W., "The Shape of Fiber Tapers," J. Lightwave Technol. 10, 432-438 (1992).

[12] Love, J. D., Henry, W. M., Stewart, W. J., Black, R. J., Lacroix, S., and Gonthier, F., "Tapered single-mode fiber devices Part 1: Adiabaticity criteria," IEE Proc.-J: Optoelectron. 138, 355-364 (1991).

[13] Zhang, K., Wang, Y., and Wu, Y.-H., "Enhanced Fano resonance in a non-adiabatic tapered fiber coupled with a microresonator," Opt. Express 42, 2956-2959 (2017).

Downloaded From: https://www.spiedigitallibrary.org/conference-proceedings-of-spie on 20 Mar 2020
Terms of Use: https://www.spiedigitallibrary.org/terms-of-use

[14] Ward, J. M., Dhasmana, N., and Nic Chormaic, S., "Hollow core, whispering gallery resonator sensors," Eur. Phys. J. Spec. Top. 223, 1917–1935 (2014).
[15] Stoian, R.-I., Bui, K. V., Rosenberger, A. T., "Silica hollow bottle resonators for use as whispering gallery mode based chemical sensors," J. Opt. 17, 125011 (2015).
[16] Rosenberger, A. T., and Rajagopal, S. R, "Enhanced dissipative sensing in a microresonator with multimode input (theory)," Proc. SPIE 11296, (in press).

Downloaded From: https://www.spiedigitallibrary.org/conference-proceedings-of-spie on 20 Mar 2020
Terms of Use: https://www.spiedigitallibrary.org/terms-of-use